NACA RM L57E23

NACA

RESEARCH MEMORANDUM

TRANSONIC FLUTTER INVESTIGATION OF A CANTILEVERED, ASPECT-RATIO-4, 45° SWEPTBACK, UNTAPERED WING WITH THREE DIFFERENT PYLON-MOUNTED EXTERNAL-STORE CONFIGURATIONS

By Charles L. Ruhlin and Robert W. Boswinkle, Jr.

Langley Aeronautical Laboratory
Langley Field, Va.

NATIONAL ADVISORY COMMITTEE
FOR AERONAUTICS
WASHINGTON
July 5, 1957

NATIONAL ADVISORY COMMITTEE FOR AERONAUTICS

RESEARCH MEMORANDUM

TRANSONIC FLUTTER INVESTIGATION OF A CANTILEVERED, ASPECT-RATIO-4, 45° SWEPTBACK, UNTAPERED WING WITH THREE DIFFERENT PYLON-MOUNTED EXTERNAL-STORE CONFIGURATIONS

By Charles L. Ruhlin and Robert W. Boswinkle, Jr.

SUMMARY

A brief, exploratory investigation has been made of the transonic flutter characteristics of a cantilevered, aspect-ratio-4, 45° sweptback, untapered wing with three different pylon-mounted external-store configurations. For stores located near the midsemispan and weighing about 0.7 of the semispan wing, the flutter speed was not changed when the store center of gravity was moved from 38 to 12 percent of the chord. The flutter speeds for these two stores were from 14 to 19 percent less than those obtained with the wings alone at subsonic speeds. The rate of rise of flutter speed with Mach number in the low supersonic range was about the same for the wing with stores as for the plain wing.

Later in the investigation, a study was made to find a store configuration which would have a substantially higher flutter speed than was obtained with the other two stores. In this study, the coupled-torsion-vibration node lines were measured for a number of stores and the one with the most forwardly located node line was selected for flutter testing. This store had about twice the mass of each of the two previous stores and was located near the tip with the store center of gravity at 25 percent of the chord ahead of the leading edge. At the subsonic Mach numbers, the flutter speed was about the same as for the wing alone. At the supersonic Mach numbers, the rate of rise of flutter speed with Mach number was higher than those for the other two stores or for the wing alone; thus, at a Mach number of 1.15 the flutter speed was 19 percent higher than for the wing alone. At a Mach number of 0.9, the value of reduced flutter speed based on the coupled-torsion-vibration frequency was lowest for the wing alone, about 2.5 times higher for the light stores, and more than 6 times higher for the heavy store.

INTRODUCTION

Numerous transonic flutter data for wings are available from investigations made in the Langley transonic blowdown tunnel (refs. 1 to 7) and in other facilities (refs. 8 to 12). These data indicate the effects of Mach number on the transonic flutter boundaries of wings which cover a wide range of wing parameters. Although the flutter of wings with stores (and concentrated weights) at subsonic speeds has received attention (for example, refs. 13 to 21) the problem at transonic speeds has been neglected in spite of the fact that the transonic regime is often a critical one for the flutter of aircraft components. In order to provide some information on the effect of stores on the transonic flutter characteristics of wings, the wing of reference 1 was selected for investigation with stores.

In the investigation the wing was cantilever-mounted and had an aspect-ratio-4, 45° sweptback, untapered plan form. Three store configurations were studied. The stores were mounted on pylons. Two of the stores, which were located near the midsemispan of the wing and had masses about 0.7 that of the wing semispan, had different chordwise locations of the centers of gravity. The third store, which was heavier and located farther outboard on the wing than the other two stores, was investigated after a study of means to obtain higher flutter speeds was made. The Mach number range extended from 0.8 to 1.3.

SYMBOLS

a — distance of wing elastic axis behind midchord measured normal to quarter-chord line in wing semichords b (Elastic axis was measured with wing clamped along a line perpendicular to leading edge and passing through intersection of wing trailing edge and root.)

A — aspect ratio of full-span wing including body intercept, $\frac{\text{Span}^2}{\text{Area}}$

A_g — aspect ratio of exposed panel of semispan wing, $\frac{(\text{Exposed semispan})^2}{\text{Exposed semispan area}}$

b — semichord of wing measured normal to quarter-chord line, ft

c — chord of wing measured streamwise, ft

d_a — streamwise distance of store leading edge ahead of wing leading edge, ft

d_b — streamwise distance of store-pylon center of gravity behind wing leading edge, ft

f_e — flutter frequency, cps

$f_{h,i}$ — natural bending vibration frequency, cps ($i = 1, 2, 3$)

f_s — coupled frequency of wing with store involving primarily side bending of store-pylon, cps

f_t — first natural torsion vibration frequency, cps

f_R — calculated flutter frequency for wing without stores, cps

f_α — uncoupled first torsion vibration frequency,

$$f_t\left(1 - \frac{x_\alpha^2/r_\alpha^2}{1 - f_{h,1}^2/f_t^2}\right)^{1/2}, \text{ cps}$$

g_h — structural damping coefficient in first bending mode

I_s — mass moment of inertia of store-pylon about wing elastic axis, slug-ft^2

I_w — mass moment of inertia of wing about wing elastic axis per unit length along quarter-chord line, slug-ft^2/ft

I_x — mass moment of inertia of store-pylon about axis through center of gravity of store-pylon and parallel to center line of store, slug-ft^2

I_y — mass moment of inertia of store-pylon about axis through store-pylon center of gravity and normal to plane of symmetry of store-pylon, slug-ft^2

k_e — reduced flutter frequency, $\dfrac{2\pi b f_e}{V_e \cos \Lambda}$

l — length of quarter-chord line of exposed wing panel, ft

m_s — mass of store-pylon, slugs

m_w — mass of wing per unit length along quarter-chord line, slugs/ft

M_e — Mach number at flutter

q_e dynamic pressure at flutter, lb/sq ft

r_α nondimensional radius of gyration of wing about wing elastic axis, $\left(\frac{I_w}{m_w b^2}\right)^{1/2}$

s wing span, ft

V_e streamwise velocity of air at flutter, ft/sec

V_R calculated streamwise velocity of air at flutter for wing without stores, ft/sec

x_{cg} distance of wing center of gravity behind wing leading edge measured normal to quarter-chord line, percent of chord normal to quarter-chord line

x_{ea} distance of wing elastic axis behind wing leading edge measured normal to quarter-chord line, percent of chord normal to quarter-chord line

x_α distance of wing center of gravity behind wing elastic axis measured normal to quarter-chord line in wing semichords b

y spanwise distance from fuselage-sting center line to plane of symmetry of store-pylon, ft

λ taper ratio of wing, $\frac{\text{Streamwise tip chord}}{\text{Chord in plane of symmetry}}$

Λ sweepback angle of wing quarter-chord line, deg

μ_e wing mass-density ratio at flutter, $\frac{m_w}{\pi \rho_e b^2}$

ρ_e air density at flutter, slugs/ft^3

MODELS

The wings used in the present investigation were constructed similar (differences are noted in the next paragraph) to those of reference 1 and are assumed to have the same properties. These properties are presented in table I. The wings had an aspect-ratio-4, 45° sweptback, taper-ratio-1.0 plan form and NACA 65A004 streamwise airfoil sections (fig. 1). Six wings were used and are designated as wings 1 to 6. Each wing was machined from a block of 2024T aluminum alloy. By using the design data of reference 22, the stiffness of each wing was reduced by perforating the plan form with a number of holes; the holes were filled with a polysulfide rubber compound, the outer surface of which was made flush with the remaining metal.

The stores had fineness ratios of 9. Each of the stores used had the same external shape which consisted of a body of revolution having an elliptical nose, a constant-diameter midsection, and a conical tail section (fig. 2(a)). Three different store configurations, each having different mass properties, were obtained by changing the internal ballast (fig. 2(b)) and are designated as store types A, B, and C. Each store was attached to the wing with pylons which were untapered, had NACA 65A005.5 streamwise airfoil sections, and were swept 45°. The pylons were constructed so that the center line of each store was parallel to the fuselage-sting center line and was located 0.25 wing chord below the wing-chord plane (figs. 1 and 3). The pylons were attached to the wing with three steel studs which passed through holes of smaller diameters (fig. 1) than those used to reduce the wing stiffness. The wings used for store types A and B had their three smaller diameter holes located exactly the same as for the wing of reference 1. The wing used for store type C had the smaller diameter holes located farther outboard.

As indicated in figure 2(b) the stores were made of balsa with lead and tungsten ballast. The pylons were made of fiber glass impregnated with a polyester-styrene-type resin. The steel studs were imbedded in the pylons and stores for attaching the store-pylons to the wings. A shell of resin-impregnated fiber glass was formed around the store-pylon to make the pylon an integral part of the store.

The parameters which describe the stores (including the pylons) are presented in table II. It should be noted (table II) that the store types A and B had different center-of-gravity locations with respect to the wing but that the spanwise and chordwise locations of the stores on the wing, the masses, and the moments of inertia of the stores about the wing elastic axis were the same, or nearly so; the stores of type C were located farther outboard on the wing and farther forward with respect to the wing leading edge, had a greater mass and moment of inertia about the wing elastic axis, and had a farther forward center-of-gravity location.

The vibration frequencies and node lines were obtained with each wing panel mounted as a cantilever to a fixed support. The measured natural vibration frequencies obtained for each wing panel without stores are given in table III(a) along with those for wing 1 of reference 1. The natural vibration frequencies obtained with stores are given in table III(b). The node lines corresponding to the first torsion and second bending frequencies of table III are presented in figure 4 along with those corresponding to the third bending frequencies for the wings without stores and for the wings with store type A. For the wings with store type B a frequency f_s was recorded (table III(b)) of a vibration mode which had a rather violent side bending motion of the store and which had the same node line as that obtained for the second bending mode. No similar store side bending modes were observed for store types A and C.

The side bending frequencies for each store type were measured with the wing clamped along the chord about 1 inch from the store both inboard and outboard of the pylon; the wing was so clamped in an attempt to remove the coupling between the wing and store. The frequencies measured for store types A, B, and C were 235, 185, and 95 cycles per second, respectively. Although the vibration modes were not charted, it was evident that the mode for store type C involved a greater amount of yawing than those for store types A and B.

TEST APPARATUS AND TECHNIQUE

The tests were made in the Langley transonic blowdown tunnel. The tunnel has a slotted, octagonal test section which measures approximately 26 inches between flats. At any predetermined Mach number up to about 1.45, a stagnation pressure of up to 75 pounds per square inch may be obtained in the test section. The tunnel is particularly useful for flutter investigations in that a constant Mach number may be maintained in the test section while the stagnation pressure, and therefore the air density, is varied. However, it should be noted that the Mach number does not uniquely define the velocity in the test section since, during the operation of the tunnel, as air in the reservoir is expended, the stagnation temperature continually decreases.

For each run (defined as one operation of the tunnel from valve opening to valve closing), the wing was clamped at an angle of attack of 0° to a 3-inch-diameter fuselage sting (figs. 1 and 5) located along the center line of the tunnel. The sting extended upstream into the subsonic flow region of the tunnel to avoid the formation of a bow shock wave from the nose of the sting. The sting had a fundamental frequency of 15 cycles per second with the model installed and weighed about 289 pounds.

Strain gages were externally mounted on the wings near the root on both top and bottom surfaces (fig. 3). An attempt was made to orient the gages so that the bending and torsion deflections of the wing could be measured separately. During each run a recording oscillograph was used to give a continuous record of the strain-gage outputs, the stagnation pressure and temperature, and the test section static pressure. The records of strain-gage outputs were used to indicate the occurrence of flutter and the flutter frequency. As an aid in determining the occurrence of flutter during a run, the output of the bending gages was circuited into the vertical component and that of the torsion gages into the horizontal component of an oscilloscope so that at flutter a Lissajous figure would appear on the scope of the instrument. A high-speed motion-picture camera was used to obtain visual records of the wing deflections during flutter for several of the runs. Models used in more than one run were checked for structural damage by visual inspection and by comparing natural vibration frequencies of the model obtained before and after each run.

More complete descriptions of the tunnel, the test procedure, and the instrumentation are given in reference 3.

RESULTS AND DISCUSSION

General Comments

In the presentation of the results, each experimental flutter speed of the wings with stores V_e has been divided by a reference flutter speed which was calculated for the wings without stores V_R. The flutter-speed ratio so formed is used in an attempt to remove the effects of air density at flutter and the effects of the small differences in wing-torsion vibration frequencies from the effects of Mach number and store configuration. The method of calculating the reference flutter speeds of the wings was the same as that used in reference 3 which was based on the method of reference 23. Briefly, the method consists of a Rayleigh-type analysis in which two-dimensional incompressible aerodynamic coefficients are used. The reduced frequencies for these coefficients are based on the velocity normal to the leading edge. The flutter-mode shape was represented by a superposition of the first and second bending and the first torsion mode shapes of a uniform cantilever beam. The measured natural first torsion vibration frequencies were uncoupled for use in the analysis by the simple formula given in the list of symbols; the measured natural bending vibration frequencies were used as the uncoupled values.

Investigation of Store Types A and B

In the initial part of the present investigation, wings with store types A and B were fluttered at Mach numbers from 0.80 to 1.29. A compilation of the experimental and analytical results for the two configurations is given in table IV and a plot of the flutter-speed ratio as a function of Mach number is presented in figure 6. The variation of flutter-speed ratio with Mach number for the wing without stores, from reference 1, is also presented in figure 6.

From the visual observation of flutter and the high-speed-camera results, the flutter obtained with store types A and B appeared to be of the bending-torsion type. The flutter frequencies were between the first-bending and first-torsion natural vibration frequencies. The flutter usually occurred with a sudden buildup from random oscillations; however, during several of the runs a low damping region (defined as a period of doubtful flutter characterized by intermittent sinusoidal oscillations of the wing) preceded or followed definite flutter. It was possible for the tunnel to operate during a given run so that the flutter boundary was intersected at more than one point, as in run 9, table IV, for example, where a start, an end, and another start of flutter were all obtained during the same run.

The flutter points obtained with store types A and B are shown to fall along a single line in figure 6. Thus, changing the static center of gravity of the stores from 38 percent of the chord (store type A) to 12 percent of the chord (store type B) appears to have no large effect on the flutter speeds. It may be noted that the mass and mass moment of inertia about the wing elastic axis for store types A and B were essentially the same.

Comparison of the flutter-speed ratios obtained with store types A and B with those obtained for the wing alone (fig. 6) indicates that addition of the stores reduced the flutter speed by 14 to 19 percent at Mach numbers below 1.0. This reduction in flutter speed seems rather small when consideration is given to the fact that the coupled torsion frequency of the wing was reduced by 60 to 70 percent with the addition of stores A and B (table III). In the absence of coupling effects of the store on the wing, the flutter speed would be expected to be nearly proportional to the torsion frequency. Since the addition of the stores reduced the flutter speed considerably less than the torsion frequency, some favorable coupling effect from both store configurations is indicated. In the low supersonic range of Mach numbers, the rate of rise of flutter-speed ratio with Mach number is seen to be about the same for the wings with and without stores.

Node-Line Survey

After obtaining the experimental results for the cantilevered wing with store configurations A and B, an attempt was made to increase the favorable coupling effect of the store. Since the flutter speed appeared to be relatively insensitive to movements of the static center-of-gravity position, at least within the limits investigated for configurations A and B, another method of qualitatively judging the coupling in terms of the flutter speed was sought.

A clue to a possible method is found in reference 24 which shows that, for the two-degree-of-freedom two-dimensional case at low speeds, a natural vibration node line at the 75-percent-chord station results in a minimum flutter speed. This theoretical result appeared to be borne out in the subsonic flutter data obtained with cantilever swept wings with stores in reference 14. An examination of the torsional node lines shown in figure 4(a) for the plain wing and for store configurations A and B indicates a relatively small difference in the node-line positions for the two store configurations, although, in comparison with the plain wing, the node lines for the store configurations are somewhat farther forward over the outer part of the wing. The assumption was therefore made that a torsional node line far forward of those of configurations A and B might be indicative of a favorable coupling effect.

Accordingly, vibration tests were made for a number of different store configurations. The vibration tests were made with store type B at six spanwise positions other than the one previously tested, at seven spanwise positions with the center of gravity of store type B moved forward, and at seven spanwise positions with store type C, which had a still farther forward center-of-gravity location (fig. 7). The node lines for the fundamental coupled torsion vibration mode obtained with each store configuration are presented in figure 8. Ratios of coupled first and second bending frequencies to the fundamental coupled torsion frequency for each of the store configurations are presented in figure 9 and table V. It may be noted that store type C at the most outboard location (fig. 8(d)) gave the most forward position of the torsion vibration node line; this store configuration was selected for flutter testing. It may also be noted that, as this store was moved along the span (fig. 9), the ratio of second bending to torsion frequency increased from a value of about 2.3 near the root to about 5 at the position used for the flutter tests.

Investigation of Store Type C

The results of the flutter tests of the wing with store type C are included in table IV and in figure 6. As with store types A and B the flutter appeared to be of the bending-torsion type and the flutter frequencies were between the first-bending and first-torsion natural frequencies; however, the flutter was of a less destructive nature than was obtained with the two previous store types. No flutter could be obtained within the dynamic-pressure range of the tunnel during three runs made at the higher supersonic Mach numbers; during one of these runs, however, low damping occurred just below and continued up to the maximum dynamic pressure obtained. The three no-flutter points are included in the results (table IV and fig. 6) to aid in drawing the flutter boundary for this configuration.

At subsonic Mach numbers the flutter-speed ratios obtained with store type C (fig. 6) were higher than those obtained with store types A and B and about the same as those obtained with the wing alone. The flutter-speed ratio increased with Mach number at a greater rate for store type C than for the other configurations; thus, the flutter boundary at low supersonic Mach numbers was considerably higher for store type C than for the wing alone or with store types A or B. It is of interest to note that, if the coupled torsional frequencies of the various configurations were used to form a reduced flutter speed $\frac{V_e}{2\pi b f_t}$, the values of reduced flutter speed at a Mach number of 0.9 would be lowest for the wing alone, would be about $2\frac{1}{2}$ times higher for store types A and B, and more than 6 times higher for store type C. Thus, for store type C a very favorable coupling effect was obtained.

CONCLUSIONS

The results of transonic flutter tests with cantilevered, aspect ratio 4, 45° sweptback, untapered wings having three different pylon-mounted external-store configurations have indicated the following:

1. The flutter speed was not changed when the store center of gravity was moved from 38 to 12 percent of the chord for stores located at about the midsemispan and weighing about 0.7 of the semispan wing. The flutter speeds for these two stores were from 14 to 19 percent less than those obtained with the wings alone at subsonic speeds. The rate of rise of flutter speed with Mach number in the low supersonic range was about the same for the wing with stores as for the plain wing.

2. A third store was investigated, which was about twice as heavy as the other two stores, was located near the wing tip, and had the farthest forward location of the coupled torsion vibration node line. The flutter speed for this store was about the same for the wing alone at subsonic Mach numbers. However, the rate of rise of flutter speed with Mach number was higher for this third store than for the other two stores or for the wing alone; thus, at a Mach number of 1.15 the flutter speed was 19 percent higher than for the wing alone.

3. At a Mach number of 0.9, the value of reduced flutter speed based on the coupled-torsion-vibration frequency was lowest for the wing alone,

about 2.5 times higher for the light stores, and more than 6 times higher for the heavy store.

Langley Aeronautical Laboratory,
National Advisory Committee for Aeronautics,
Langley Field, Va., May 1, 1957.

REFERENCES

1. Ruhlin, Charles L.: Experimental Transonic Flutter Characteristics of an Untapered, 45° Sweptback, Aspect-Ratio-4 Wing. NACA RM L55L22, 1956.

2. Bursnall, William J.: Initial Flutter Tests in the Langley Transonic Blowdown Tunnel and Comparison With Free-Flight Flutter Results. NACA RM L52K14, 1953.

3. Unangst, John R., and Jones, George W., Jr.: Some Effects of Sweep and Aspect Ratio on the Transonic Flutter Characteristics of a Series of Thin Cantilever Wings Having a Taper Ratio of 0.6. NACA RM L55I13a, 1956.

4. Jones, George W., Jr., and Unangst, John R.: Investigation To Determine Effects of Center-of-Gravity Location on Transonic Flutter Characteristics of a 45° Sweptback Wing. NACA RM L55K30, 1955.

5. Land, Norman S., and Abbott, Frank T., Jr.: Transonic Flutter Investigation of a Fighter-Airplane Wing Model and Comparison With a Systematic Plan-Form Series. NACA RM L55B16, 1955.

6. Jones, George W., Jr., and Young, Lou S., Jr.: Transonic Flutter Investigation of Two 64° Delta Wings With Simulated Streamwise Rib and Orthogonal Spar Construction. NACA RM L56I27, 1957.

7. Jones, George W., Jr.: Investigation of Transonic Flutter Characteristics of a Thin 10° Sweptback Wing Having an Aspect Ratio of 4 and a Taper Ratio of 0.6. NACA RM L56L14a, 1957.

8. Herrera, Raymond, and Barnes, Robert H.: An Experimental Investigation of the Flutter of Several Wings of Varying Aspect Ratio, Density, and Thickness Ratio at Mach Numbers From 0.60 to 1.10. NACA RM A54A29, 1954.

9. Warner, Robert W.: Comparison Between Analytical and Wind-Tunnel Results on Flutter of Several Low-Aspect-Ratio, High-Density, Unswept Wings at High Subsonic Speeds and Zero Angle of Attack. NACA RM A55G08, 1955.

10. Pratt, George L.: Experimental Flutter Investigation of a Thin Unswept Wing at Transonic Speeds. NACA RM L55A18, 1955.

11. Maier, H. G., and King, S. R.: Special Progress Report. The Critical Flutter Mach Number for 45° Sweptback Wings - Transonic Flutter Model Test. Report No. C.A.L.-70 (Contract No. AF33(616)-179), Cornell Aero. Lab., Inc., Jan. 1955.

12. Lauten, William T., Jr., and Burgess, Marvin S.: Flutter Investigation in the High Subsonic and Transonic Speed Range on Cantilever Delta-Wing Planforms With Leading-Edge Sweepback of 60°, 53° 8', and 45°. NACA RM L56K26, 1957.

13. Brady, W. G., Loewy, R. G., and Targoff, W. P.: Subsonic Flutter Model Tests of Wings Carrying Heavy Tip Pods. Pt. 1. Straight Wings. WADC Tech. Rep. 53-161. Wright Air Div. Center, U. S. Air Force, July 1954.

14. Brady, W. G., Maier, H. G., and Targoff, Walter P.: Subsonic Flutter Model Tests of Wings Carrying Heavy Tip Pods. Pt. 2. Swept Wings. WADC Tech. Rep. 53-161, Wright Air Div. Center, U. S. Air Force, Nov. 1954.

15. Runyan, Harry L., and Sewall, John L.: Experimental Investigation of the Effects of Concentrated Weights on Flutter Characteristics of a Straight Cantilever Wing. NACA TN 1594, 1948.

16. Sewall, John L., and Woolston, Donald S.: Preliminary Experimental Investigation of Effects of Aerodynamic Shape of Concentrated Weights on Flutter of a Straight Cantilever Wing. NACA RM L9E17, 1949.

17. Nelson, Herbert C., and Tomassoni, John E.: Experimental Investigation of the Effects of Sweepback on the Flutter of a Uniform Cantilever Wing With a Variably Located Concentrated Mass. NACA RM L9F24, 1949.

18. Tomassoni, John E., and Nelson, Herbert C.: Experimental Investigation of the Effects of Root Restraint on the Flutter of a Sweptback, Uniform, Cantilever Wing With a Variably Located Concentrated Mass. NACA RM L9J21a, 1950.

19. Sewall, John L.: Experimental and Analytical Investigation of Flutter of a Nonuniform Sweptback Cantilever Wing With Two Concentrated Weights. NACA RM L51H09a, 1951.

20. Gaukroger, D. R.: A Theoretical Treatment of the Flutter of a Wing With a Localised Mass. Rep. No. Structures 213, British R.A.E., Aug. 1956.

21. Martina, Albert P.: Flutter Investigation at Low Speed of a 40° Sweptback Wing With Pylon-Mounted Stores, Tested as a Semispan-Cantilever Wing and as a Full-Span Wing on a Towed Airplane Model. NACA RM L56F14a, 1956.

[redacted]

22. Land, Norman S., and Abbott, Frank T., Jr.: Method of Controlling Stiffness Properties of a Solid-Construction Model Wing. NACA TN 3423, 1955.

23. Barmby, J. G., Cunningham, H. J., and Garrick, I. E.: Study of Effects of Sweep on the Flutter of Cantilever Wings. NACA Rep. 1014, 1951. (Supersedes NACA TN 2121.)

24. Biot, M. A., and Arnold, Lee: Low-Speed Flutter and Its Physical Interpretation. Jour. Aero. Sci., vol. 15, no. 4, Apr. 1948, pp. 232-236.

TABLE I.- WING PROPERTIES

Streamwise airfoil section	NACA 65A004
A	4
Λ, deg	45
λ	1.0
A_g	1.57
c, ft	0.292
s, ft	1.166
b, ft	0.103
l, ft	0.648
m_w, slug/ft	6.77×10^{-3}
I_w, slug-ft^2/ft	18.0×10^{-6}
x_{ea}	42.5
x_{cg}	44.8
x_α	0.05
a	-0.15
$r_\alpha^{\,2}$	0.25
g_h	0.007

TABLE II.- STORE PROPERTIES AND LOCATIONS

Store type	$\frac{2y}{s}$	$\frac{d_a}{c}$	$\frac{d_b}{c}$	$\frac{m_s}{l m_w}$	$\frac{I_s}{l I_w}$	I_x, slug-ft^2	I_y, slug-ft^2
A	0.636	0.60	0.38	0.72	3.9	2.18×10^{-6}	54.3×10^{-6}
B	.636	.60	.12	.73	4.0	2.27	31.2
C	.893	.77	-.25	1.42	15.5	2.82	54.5

TABLE III.- VIBRATION FREQUENCIES OF WINGS WITH AND WITHOUT STORES

(a) Without stores

Wing	1		2		3		4		5		6		1 of reference 1
Panel	Left	Right	Left	Right	Left	Right	Left	Right	Left	Right	Left	Right	Semispan model
$f_{h,1}$, cps	42.3	40.8	40.7	42.0	42.0	42.0	43.0	43.0	40.9	42.5	41.2	42.5	42.3
$f_{h,2}$, cps	243	240	238	243	242	243	252	255	238	247	241	247	240
$f_{h,3}$, cps	658	661	650	655	652	655	674	678	643	669	650	669	650
f_t, cps	382	374	383	377	374	377	393	393	376	385	380	385	376
$f_{h,1}/f_t$	.111	.109	.106	.111	.112	.111	.109	.109	.109	.110	.108	.110	.112
$f_{h,2}/f_t$	.636	.642	.621	.645	.647	.645	.641	.649	.633	.642	.634	.642	.638
f_α, cps	380.1	372.1	381.1	375.1	372.1	375.1	391.0	391.0	374.1	383.0	378.4	383.0	374.4

(b) With stores

Store type	A						B				C	
Wing	1		2		3		4		5		6	
Panel	Left	Right	Left	Right	Left	Right	Left	Right	Left	Right	Left	Right
$f_{h,1}$, cps	35.0	34.0	34.4	35.0	34.8	35.0	38.7	39.0	36.1	37.6	24.8	25.0
$f_{h,2}$, cps	194	193	187	192	188	192	243	244	241	248	288	288
f_t, cps	131	127	124	129	130	129	117	118	107	117	59.5	59.0
f_s, cps	-------	-------	-------	-------	-------	-------	188	189	186	193	-------	-------
$f_{h,1}/f_t$	.267	.268	.277	.271	.268	.271	.331	.330	.337	.321	.417	.424
$f_{h,2}/f_t$	1.481	1.520	1.508	1.488	1.446	1.488	2.077	2.068	2.252	2.120	4.840	4.881

TABLE IV.- COMPILATION OF RESULTS

Store type	Wing	Run	Point	Wing behavior[1] Left	Right	M_e	$\frac{V_e}{V_R}$	μ_e	V_e	ρ_e	q_e	f_e	$\frac{f_e}{f_R}$	k_e
A	1	1	1	N	D_1	0.768	0.860	61.67	801.3	0.0033	1058.4	117	0.8440	0.1336
	1	1	2	D_1	D_1	.790	.888	59.95	820.6	.0034	1141.9	106	.7577	.1182
	1	1	3	F_1	F_1	.801	.902	59.12	830.9	.0034	1188.0	88	.6276	.0969
	2	2	1	F_1	F_1	.849	.892	71.57	876.9	.0028	1093.0	90	.6748	.0938
	2	3	1	F_1	G	.884	.862	94.57	929.2	.0021	927.4	77	.6349	.0759
	2	4	1	F_1	F_1	.891	.885	86.84	928.1	.0023	1008.0	78	.6275	.0769
	3	5	1	F_1	D_1	1.282	1.157	93.48	1228.5	.0022	1643.0	107	.8893	.0797
B	4	6	1	F_1	F_1	.799	.877	57.94	834.3	.0035	1221.1	93	.6344	.1020
	5	7	1	F_1	F_1	.916	.878	95.72	951.8	.0021	963.4	79	.6548	.0759
	5	8	1	F_1	N	.945	.855	113.73	982.7	.0018	864.0	71	.6337	.0661
	5	8	2	EF_1	N	.999	.890	115.74	1029.5	.0018	931.7	71	.6382	.0631
	5	8	3	ED_1	N	1.085	.933	121.41	1097.6	.0017	1009.4	78	.7154	.0650
	5	9	1	F_1	F_1	.945	.855	113.99	983.8	.0018	864.0	72	.6426	.0669
	5	9	2	EF_1	EF_1	.972	.872	115.41	1007.6	.0018	894.2	72	.6472	.0653
	5	9	3	ED_1	N	1.084	.940	119.00	1098.1	.0017	1029.6	78	.7082	.0650
	5	9	4	F_2	N	1.288	1.178	86.36	1233.0	.0024	1789.9	95	.7565	.0705
C	6	10	1	F_1	N	.859	1.081	37.62	879.7	.0054	2115.4	46	.2916	.0477
	6	10	2	F_1	F_1	.873	1.107	36.27	892.1	.0056	2246.4	47	.2953	.0480
	6	11	1	F_1	F_1	.899	1.010	54.90	918.9	.0037	1582.6	44	.3041	.0441
	6	12	1	F_1	N	.908	1.042	46.16	899.3	.0044	1800.0	44	.2910	.0445
	6	13	1	F_1	F_1	.924	.974	65.52	936.8	.0031	1379.5	42	.3047	.0412
	6	14	1	F_1	F_1	.944	1.020	59.74	953.0	.0034	1559.5	44	.3106	.0419
	6	15	1	D_1	D_1	.966	.993	72.54	986.9	.0028	1393.9	42	.3145	.0387
	6	15	2	F_1	F_1	1.037	1.077	61.55	1016.2	.0033	1702.1	42	.2999	.0383
	6	16	1	F_1	N	1.123	1.206	58.04	1116.9	.0035	2207.5	43	.3012	.0356
	6	16	2	F_1	F_1	1.056	1.178	50.78	1047.4	.0040	2181.6	45	.3047	.0391
	6	17	1	D_1	N	1.175	1.311	47.24	1139.8	.0043	2815.2	44	.2926	.0356
	6	17	2	D_1	M	1.172	1.408	30.32	1081.3	.0067	3929.8	48	.2920	.0407
	6	18	1	M	M	1.190	1.441	30.32	1106.5	.0067	4121.3	---	------	------
	6	19	1	M	M	1.298	1.443	43.22	1221.9	.0047	3532.0	---	------	------

[1] The following code identifies the wing behavior at the various data points.

D	low damping	G	strain gages not functioning
ED	end of low damping which followed definite flutter	M	maximum dynamic pressure obtained with no flutter
EF	end of definite flutter	N	no flutter or low damping
F	definite flutter	1, 2	associated with first or second occurrence, respectively, of flutter during a run; used as subscript

[redacted]

TABLE V.- MEASURED VIBRATION FREQUENCIES OF WING WITH STORES AT VARIOUS SPANWISE LOCATIONS

Store type	Store center-of-gravity chordwise location	Store spanwise location, 2y/s	$f_{h,1}$, cps	$f_{h,2}$, cps	f_t, cps	f_s, cps	$f_{h,1}/f_t$	$f_{h,2}/f_t$
A	0.38c behind wing leading edge	0.636	35	190	127	---	0.27	1.48
B	0.12c behind wing leading edge	.378	44	240	175	---	.25	1.37
		.464	43	240	150	---	.29	1.60
		.550	41	215	125	---	.33	1.72
		.636	38	250	112	185	.34	2.23
		.721	35	300	103	175	.34	2.91
		.807	31	320	98	165	.32	3.26
		.893	26	330	95	155	.28	3.47
B	0.05c ahead of wing leading edge	.378	44	245	175	---	.25	1.40
		.464	44	245	150	---	.29	1.63
		.550	42	230	120	---	.35	1.92
		.636	40	250	105	---	.38	2.38
		.721	36	290	94	185	.38	3.08
		.807	32	320	90	170	.36	3.56
		.893	28	330	87	165	.33	3.79
C	0.25c ahead of wing leading edge	.378	44	238	106	---	.42	2.25
		.464	43	230	89	---	.48	2.58
		.550	41	215	73	---	.57	2.94
		.636	38	230	62	---	.62	3.71
		.721	34	262	58	---	.59	4.52
		.807	29	280	58	---	.50	4.83
		.893	24	285	58	---	.41	4.91

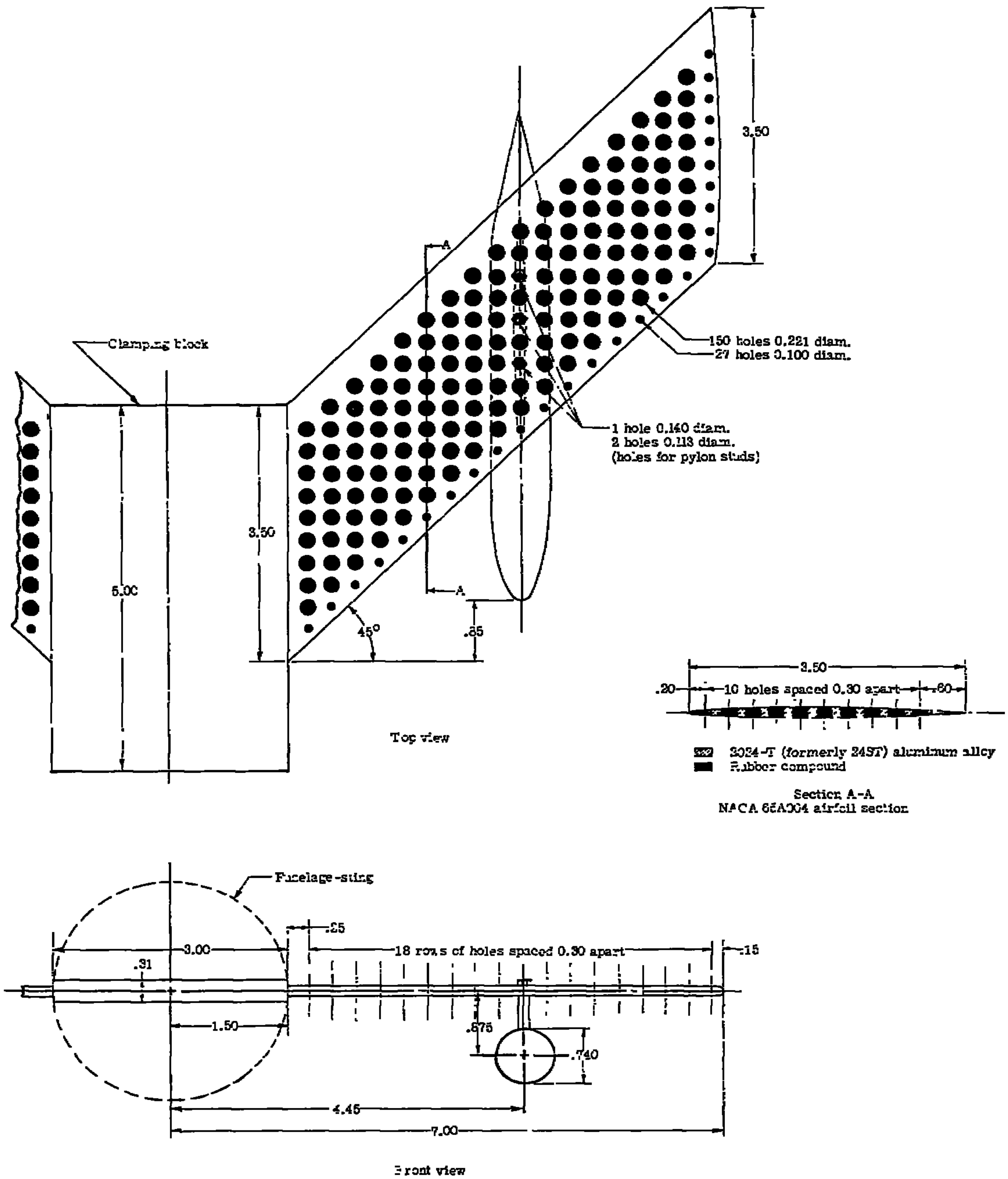

(a) Wing with store type A or B.

Figure 1.- Sketches of models. All dimensions are in inches.

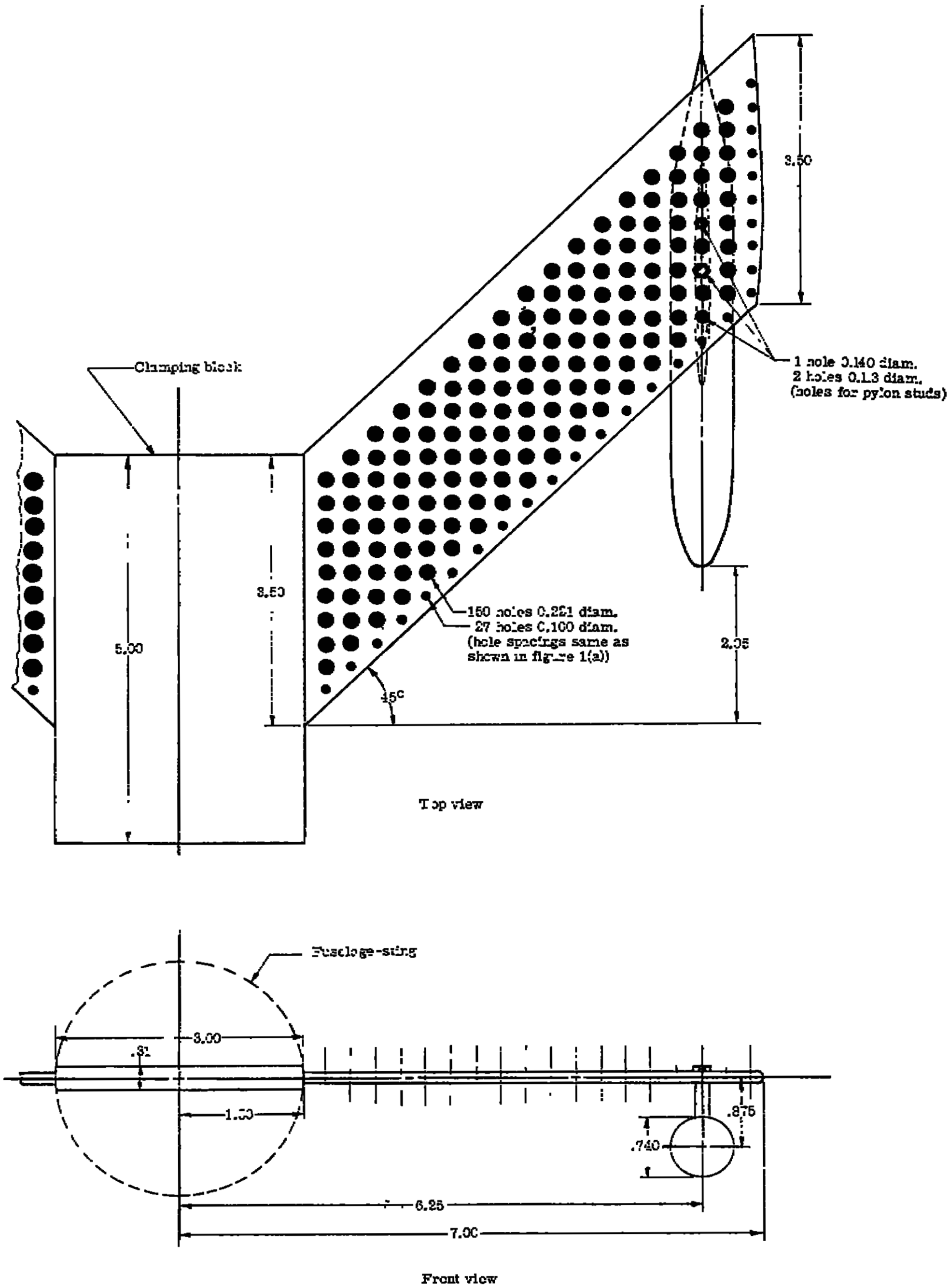

(b) Wing with store type C.

Figure 1.- Concluded.

Ordinates of store body	
Distance from nose	Radius
0	0
.014	.051
.064	.108
.214	.192
.464	.269
.714	.317
.964	.347
1.214	.364
1.482	.370
4.446	.370
4.714	.364
4.964	.347
5.214	.317
5.464	.269
6.669	0

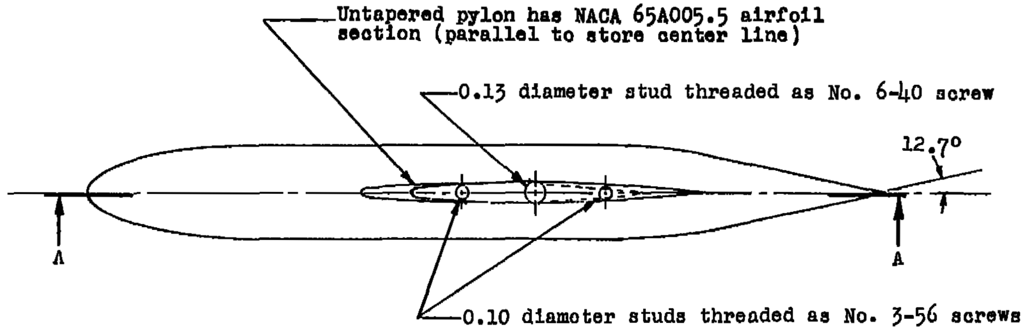

Top view

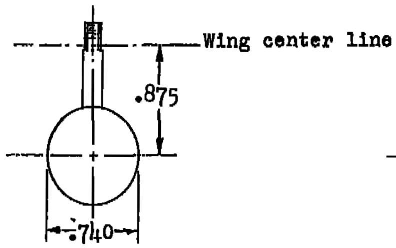

Front view

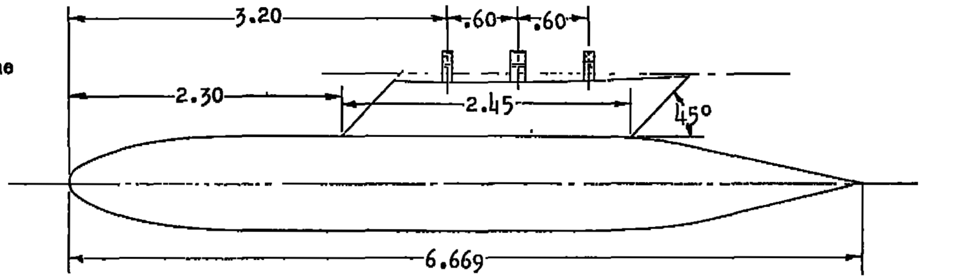

Side view

(a) General store dimensions. Sectional view A-A shown in figure 2(b).

Figure 2.- Sketch of model stores. All dimensions are in inches.

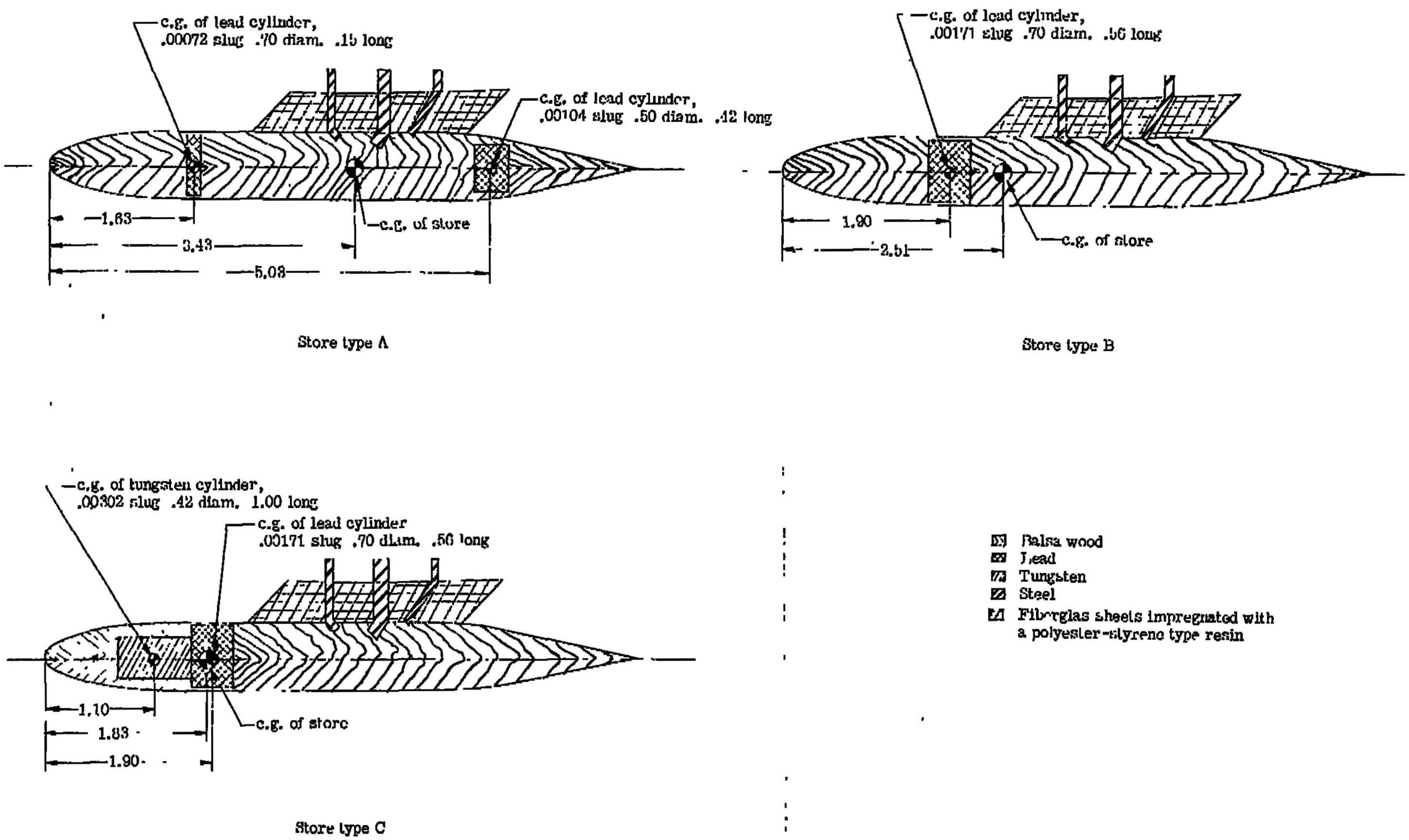

(b) Sectional view A-A showing details of construction of stores. Stores were covered by approximately 0.02 thick layer of fiber glass sheets impregnated with a polyester-styrene type resin.

Figure 2.- Concluded.

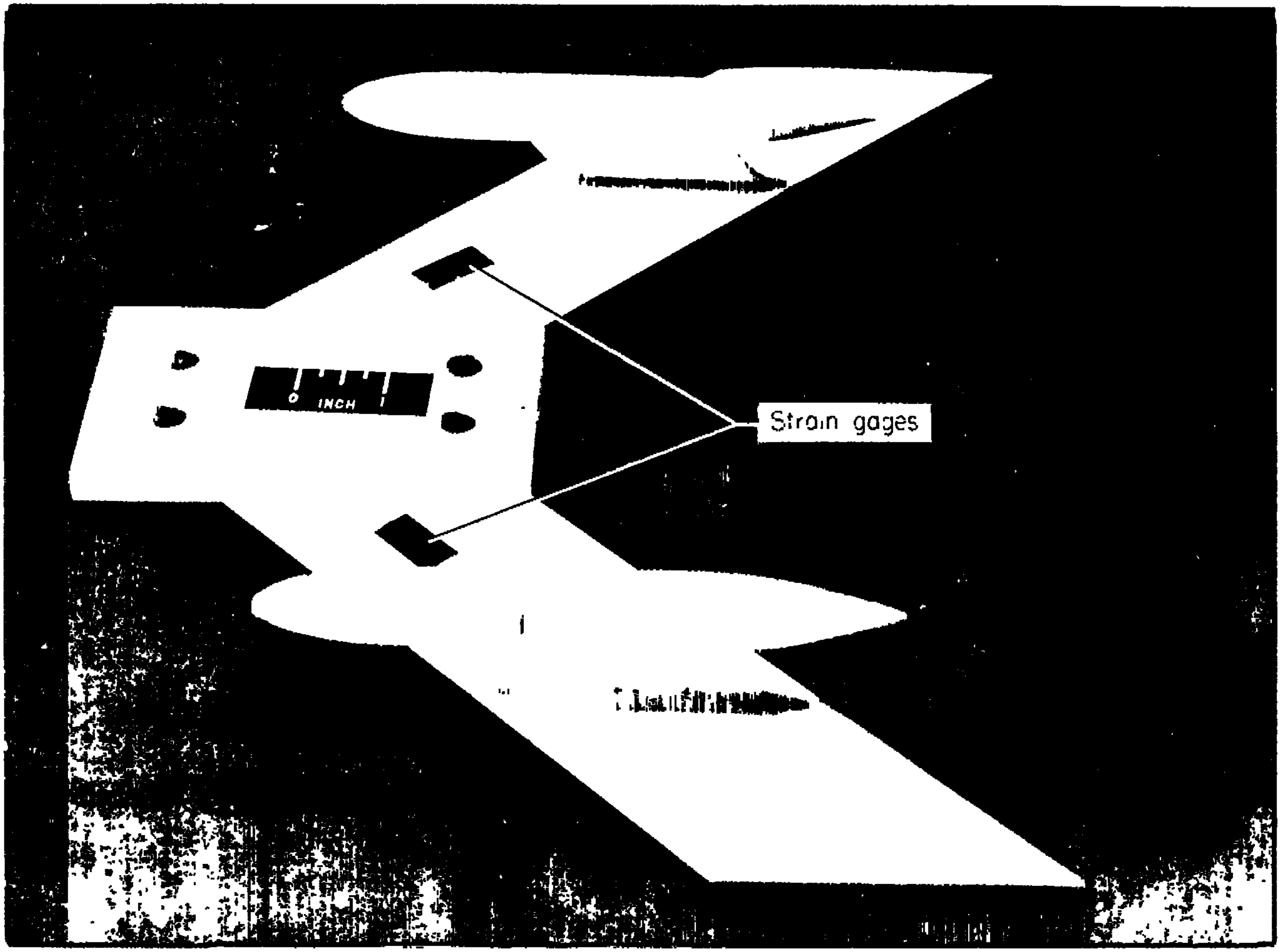

L-92878.1

(a) Underside view of wing with store type A or B.

Figure 3.- Photographs of models.

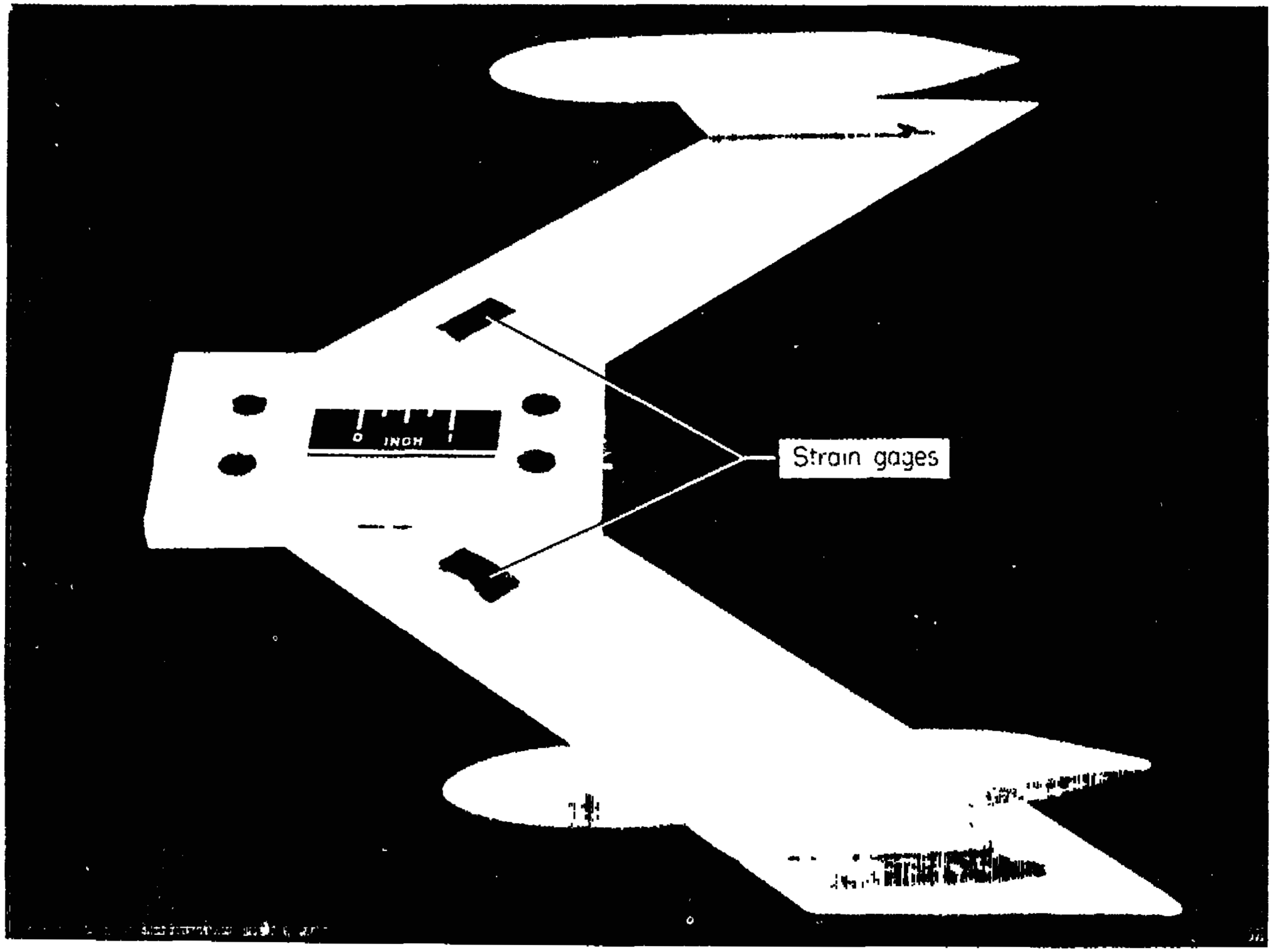

(b) Underside view of wing with store type C. L-92879.1

Figure 3.- Concluded.

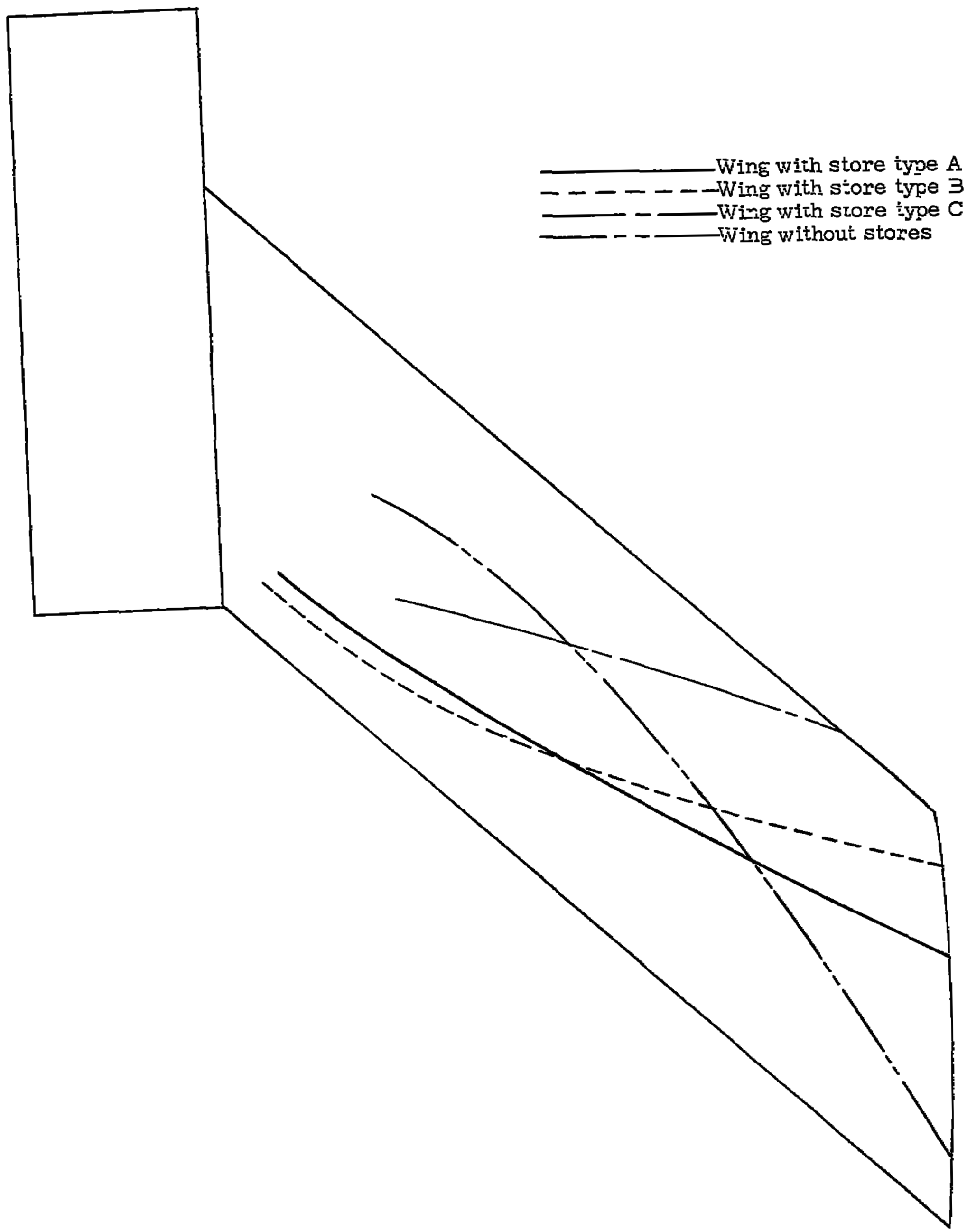

(a) First torsion mode.

Figure 4.- Natural vibration node lines.

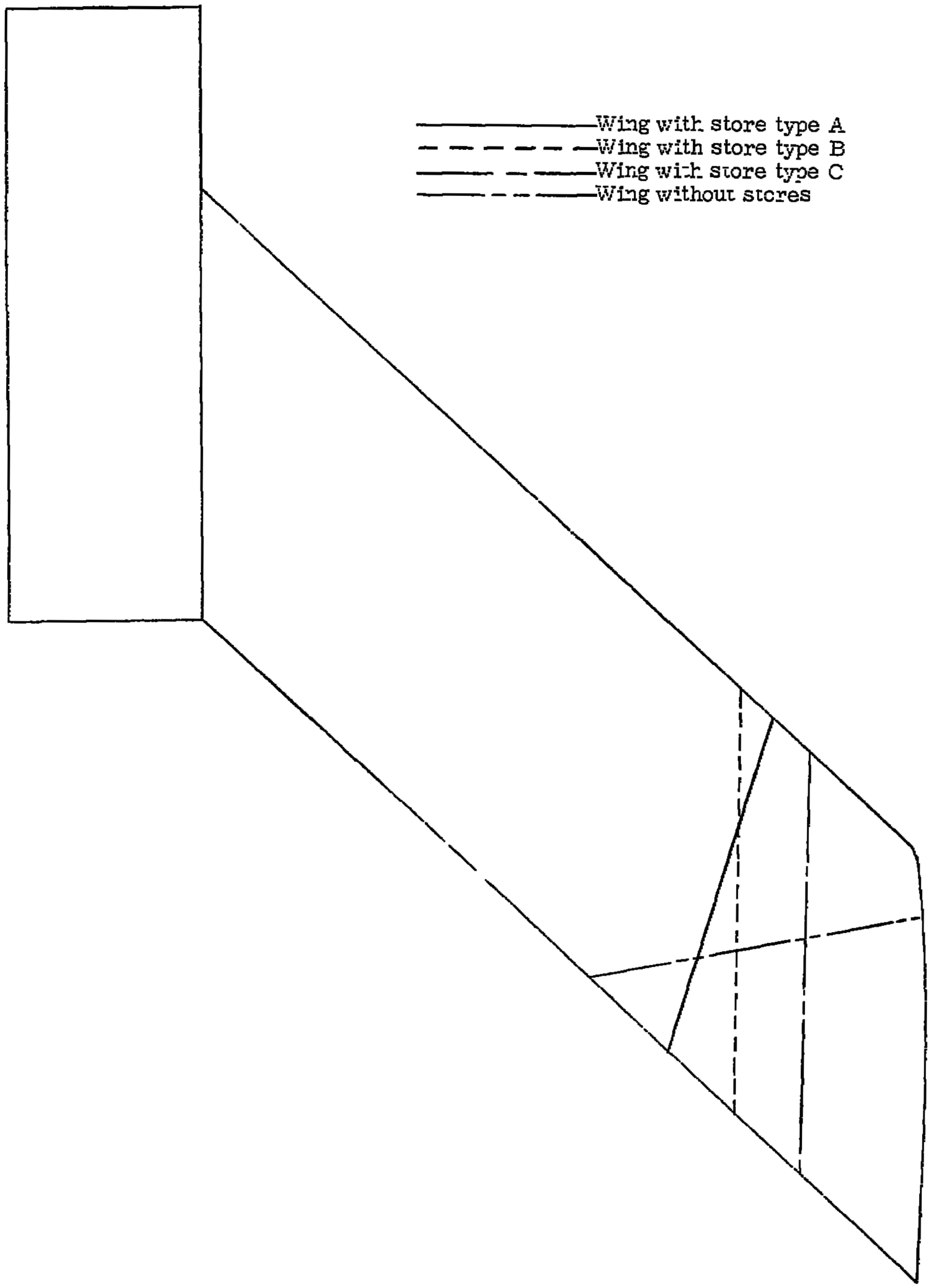

(b) Second bending mode.

Figure 4.- Continued.

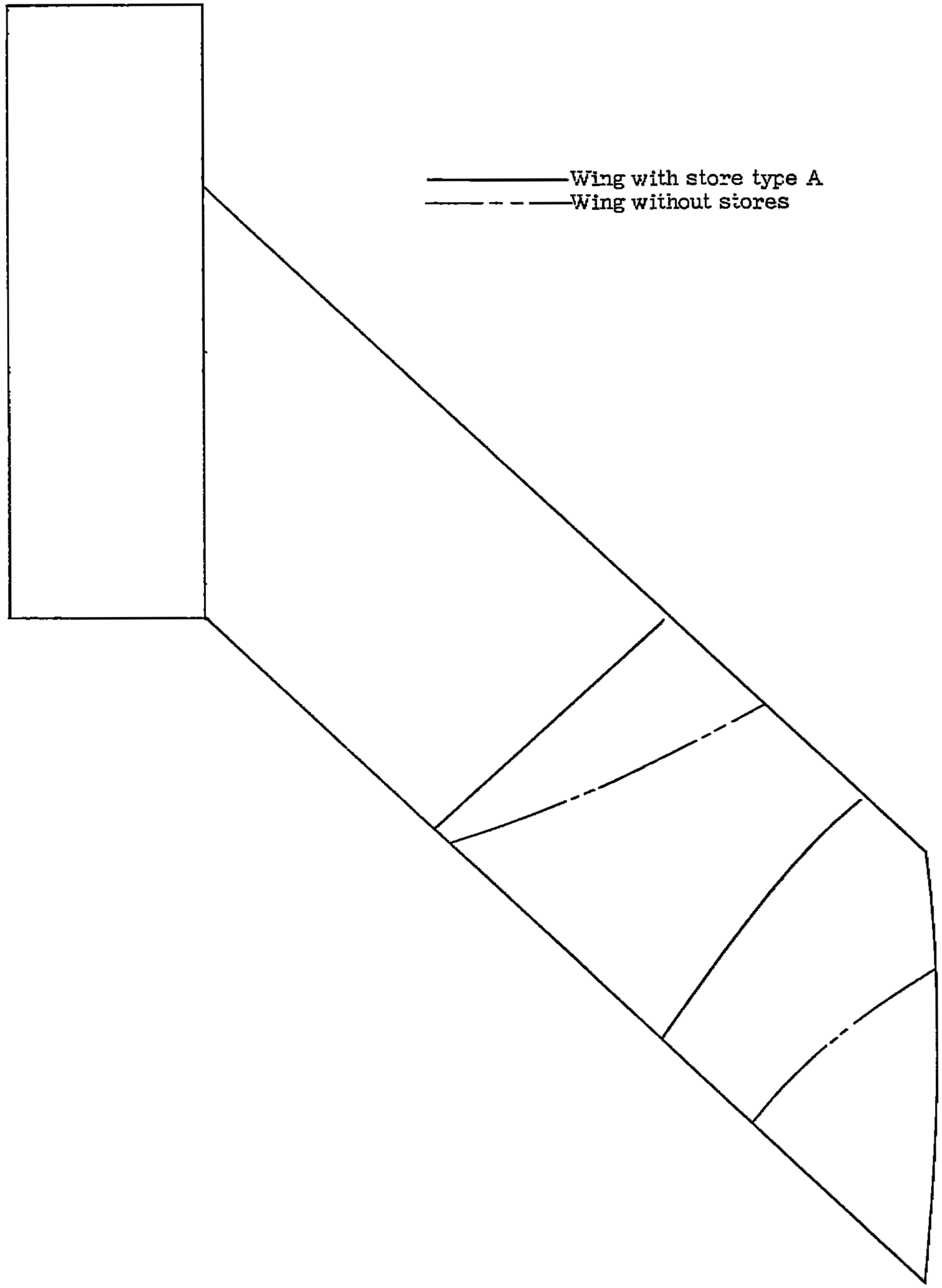

(c) Third bending mode.

Figure 4.- Concluded.

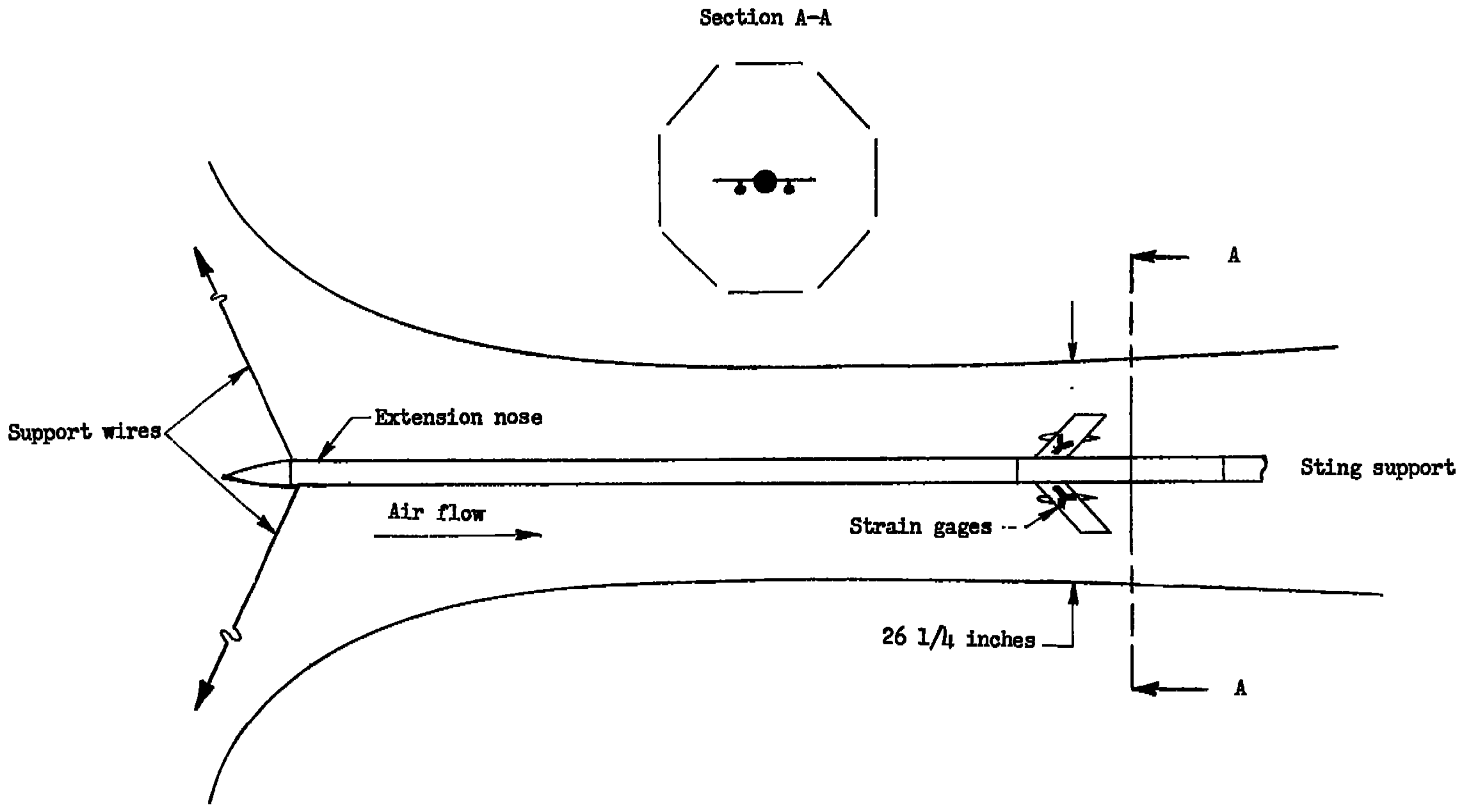

Figure 5.- Plan view of Langley transonic blowdown tunnel showing model wing with store type A or B installed.

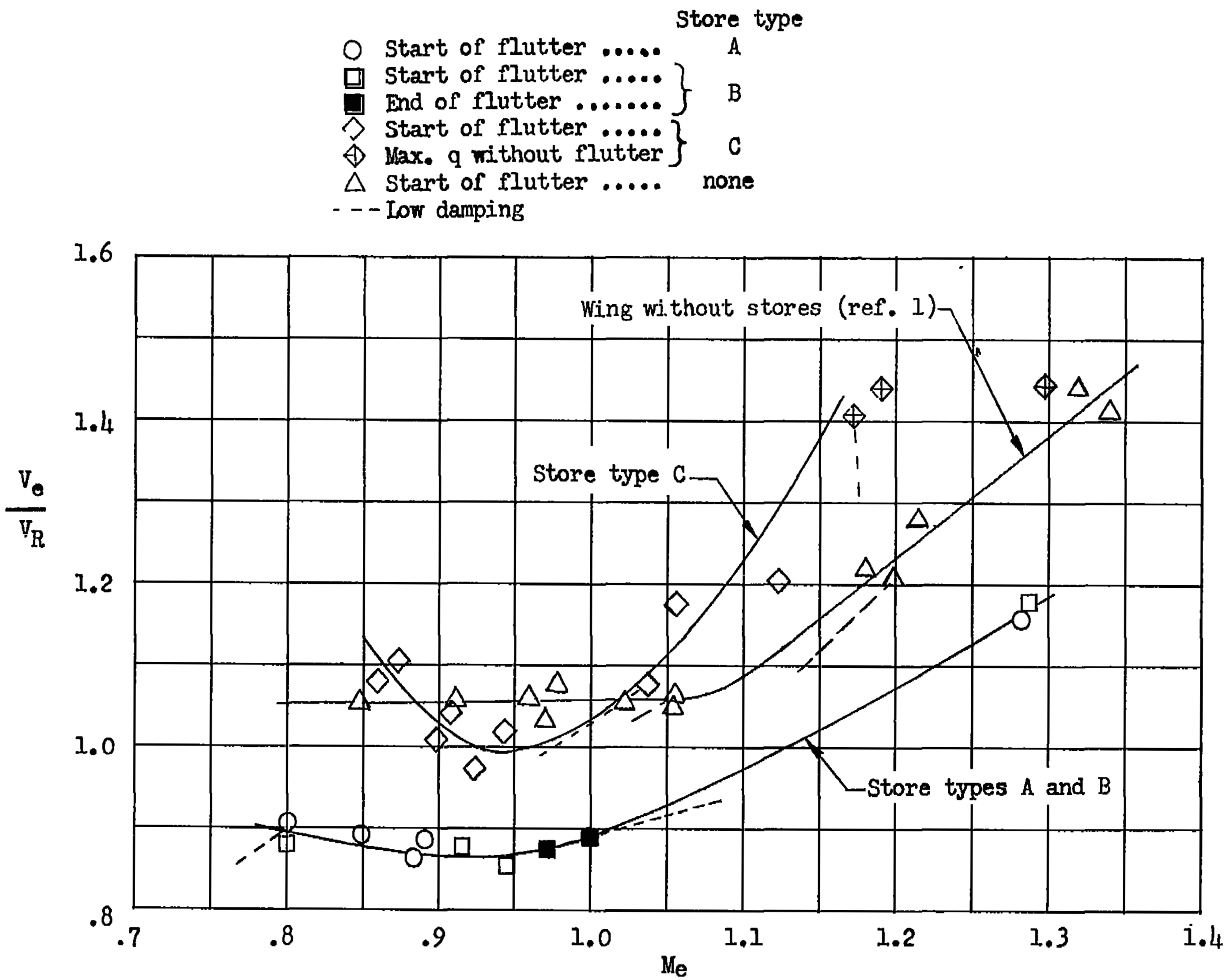

Figure 6.- Variation of flutter-speed ratio with Mach number for wing with and without stores.

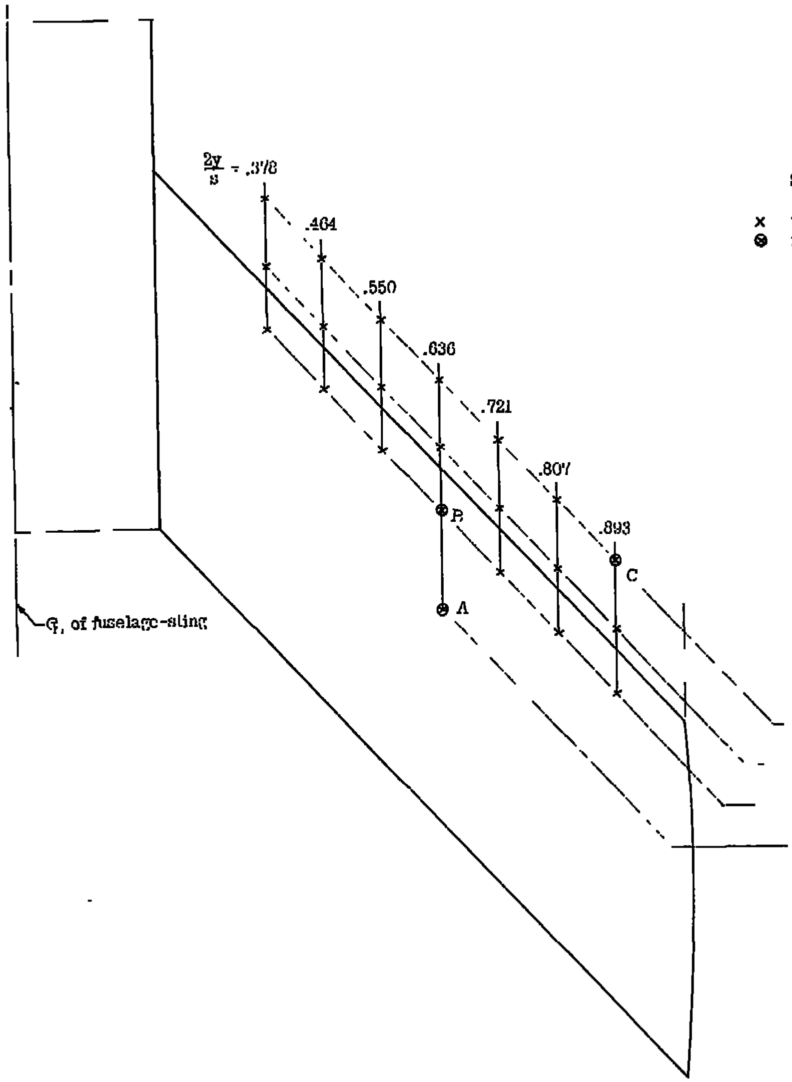

$\frac{d_a}{c}$	$\frac{d_b}{c}$	Store type	$\frac{m_s}{i m_w}$	$\frac{I_s}{i I_w}$
0.77	-0.248	C	1.42	15.5
.77	-.054	B	.73	5.6
.60	.117	B	.73	4.0
.60	.380	A	.72	3.9

Figure 7.- Store-pylon center-of-gravity locations at which vibration surveys and flutter tests were made.

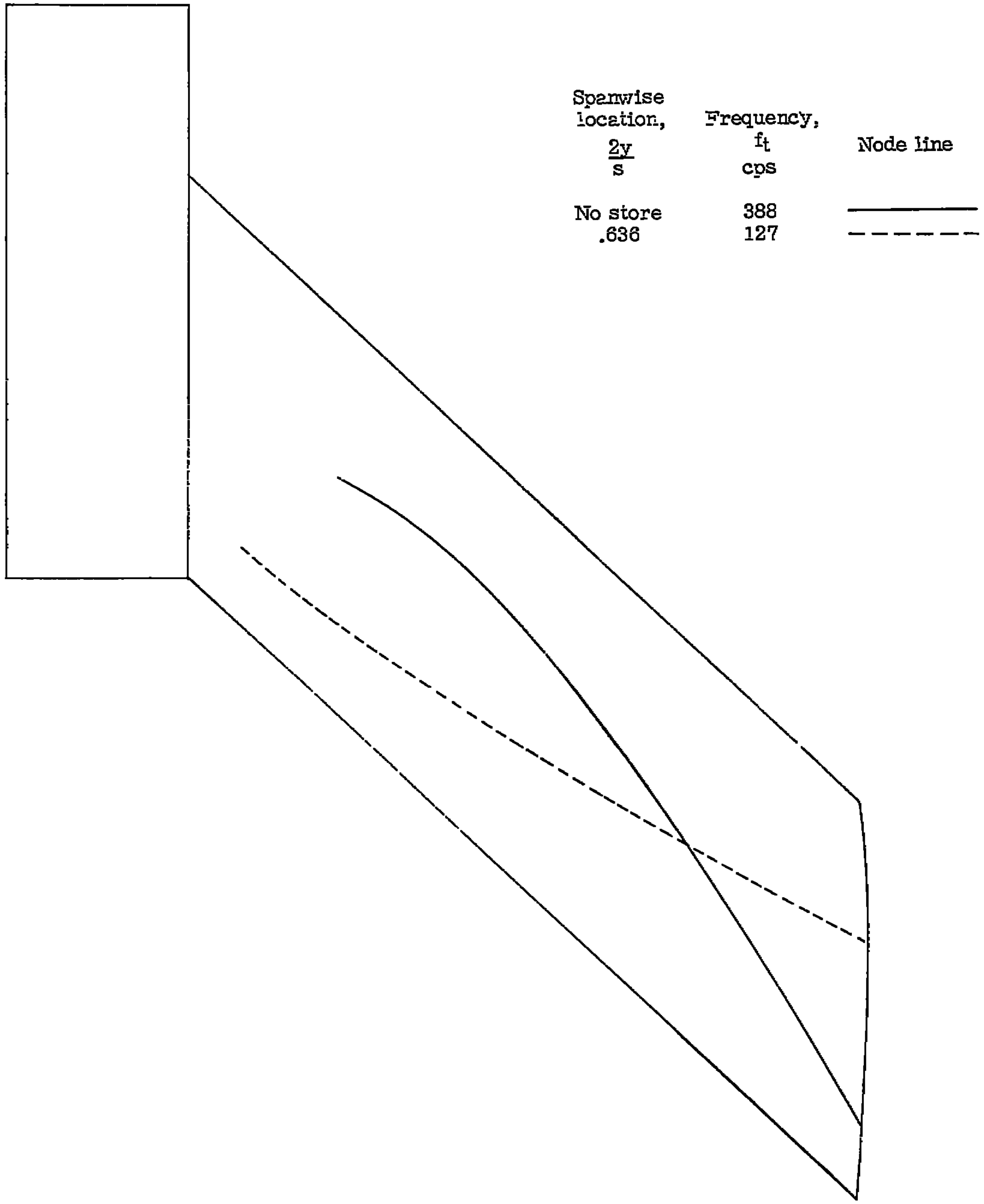

(a) Center of gravity of store-pylon type A at 0.380c behind wing leading edge.

Figure 8.- Measured coupled torsion frequencies and node lines with the stores at various spanwise locations.

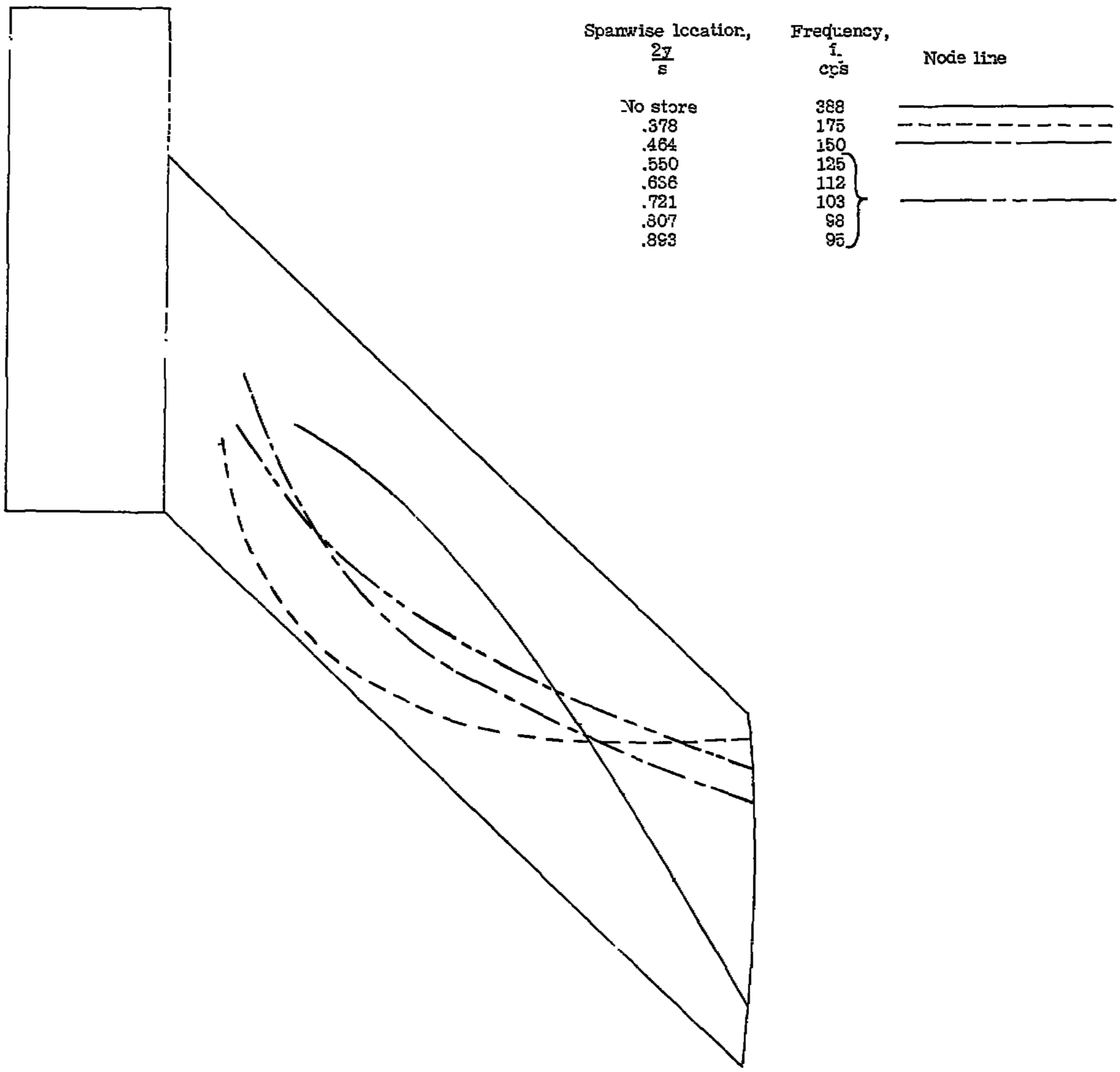

(b) Center of gravity of store-pylon type B at 0.117c behind wing leading edge.

Figure 8.- Continued.

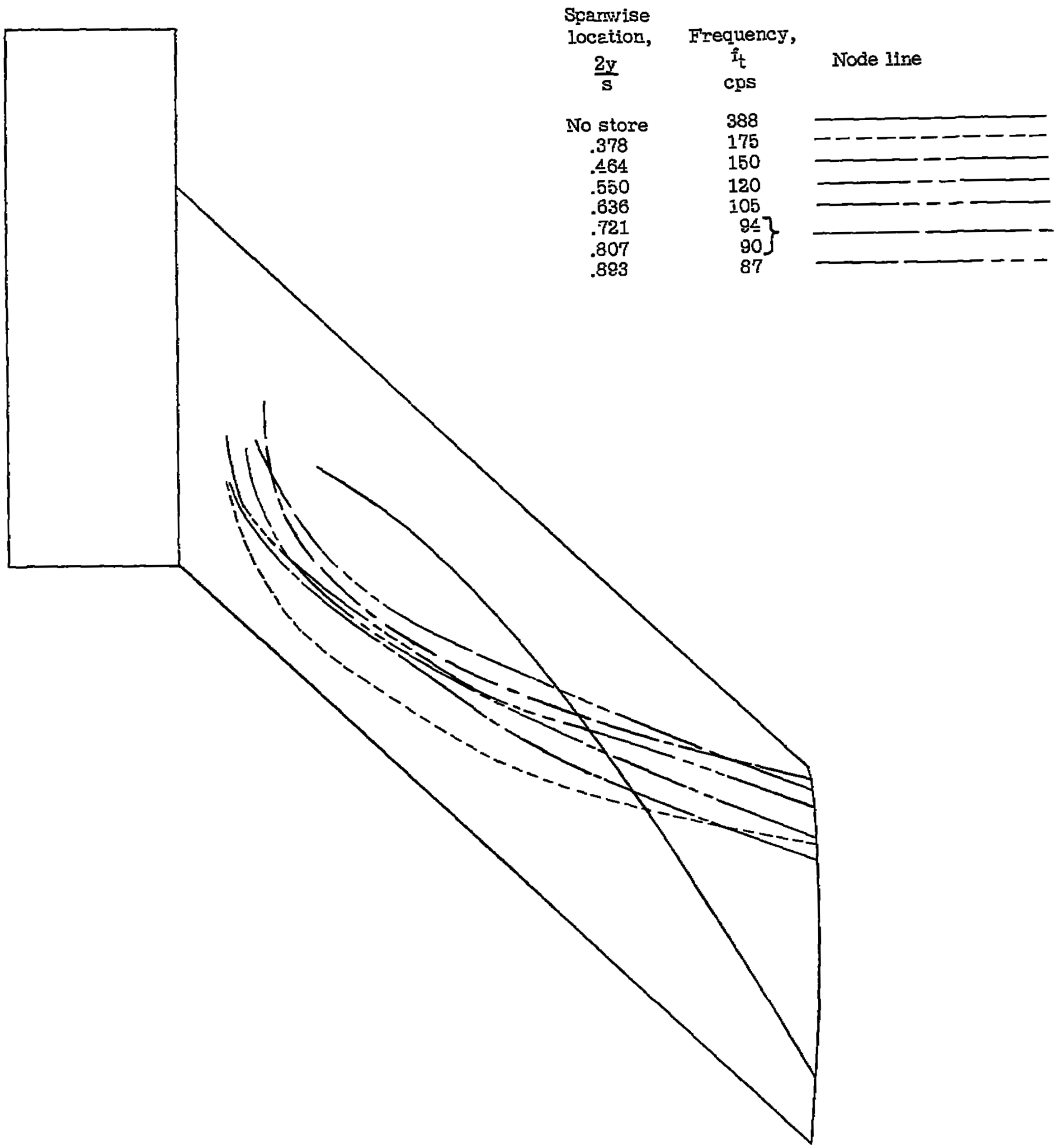

(c) Center of gravity of store-pylon type B at 0.054c ahead of wing leading edge.

Figure 8.- Continued.

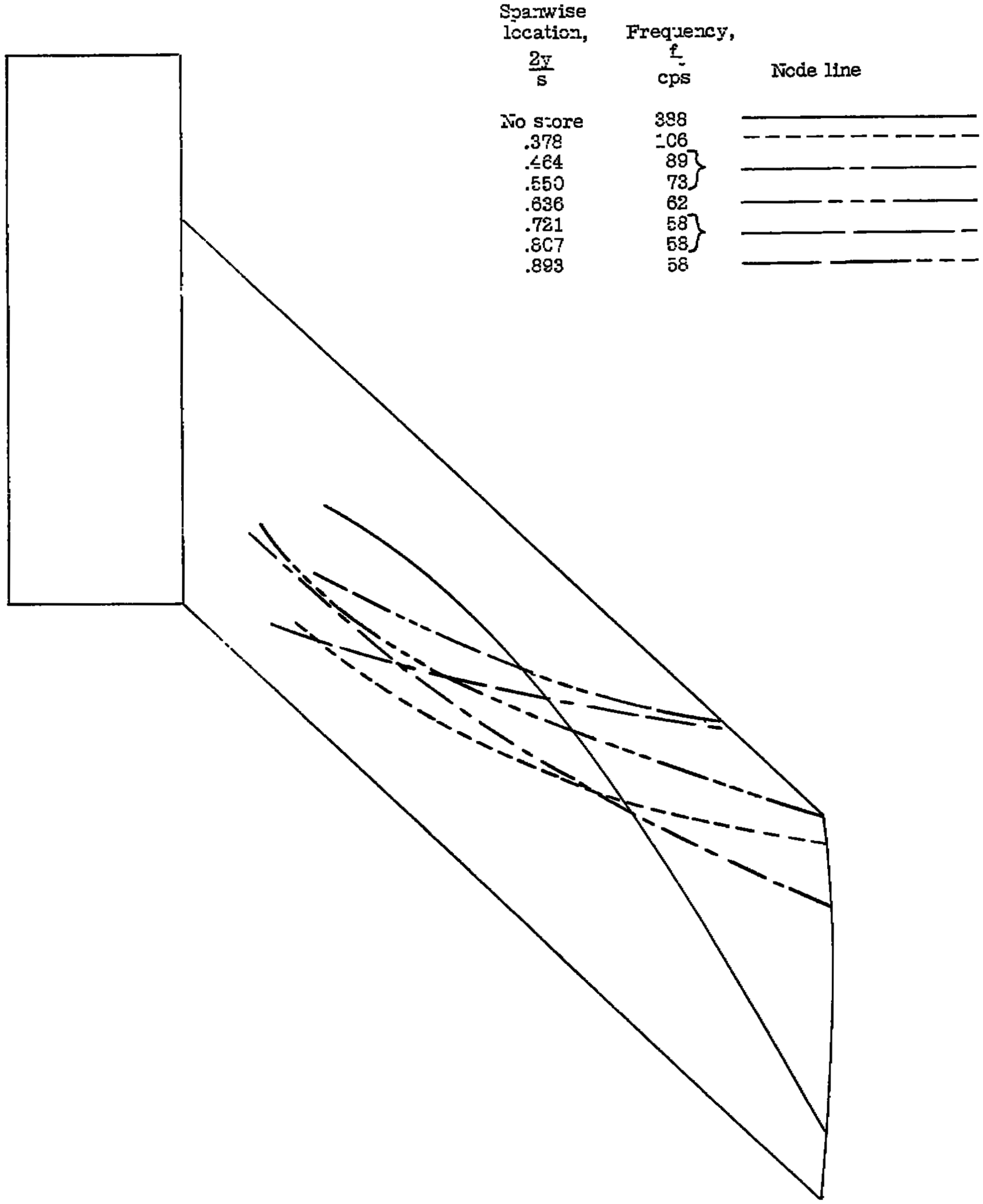

(d) Center of gravity of store-pylon type C at 0.248c ahead of wing leading edge.

Figure 8.- Concluded.

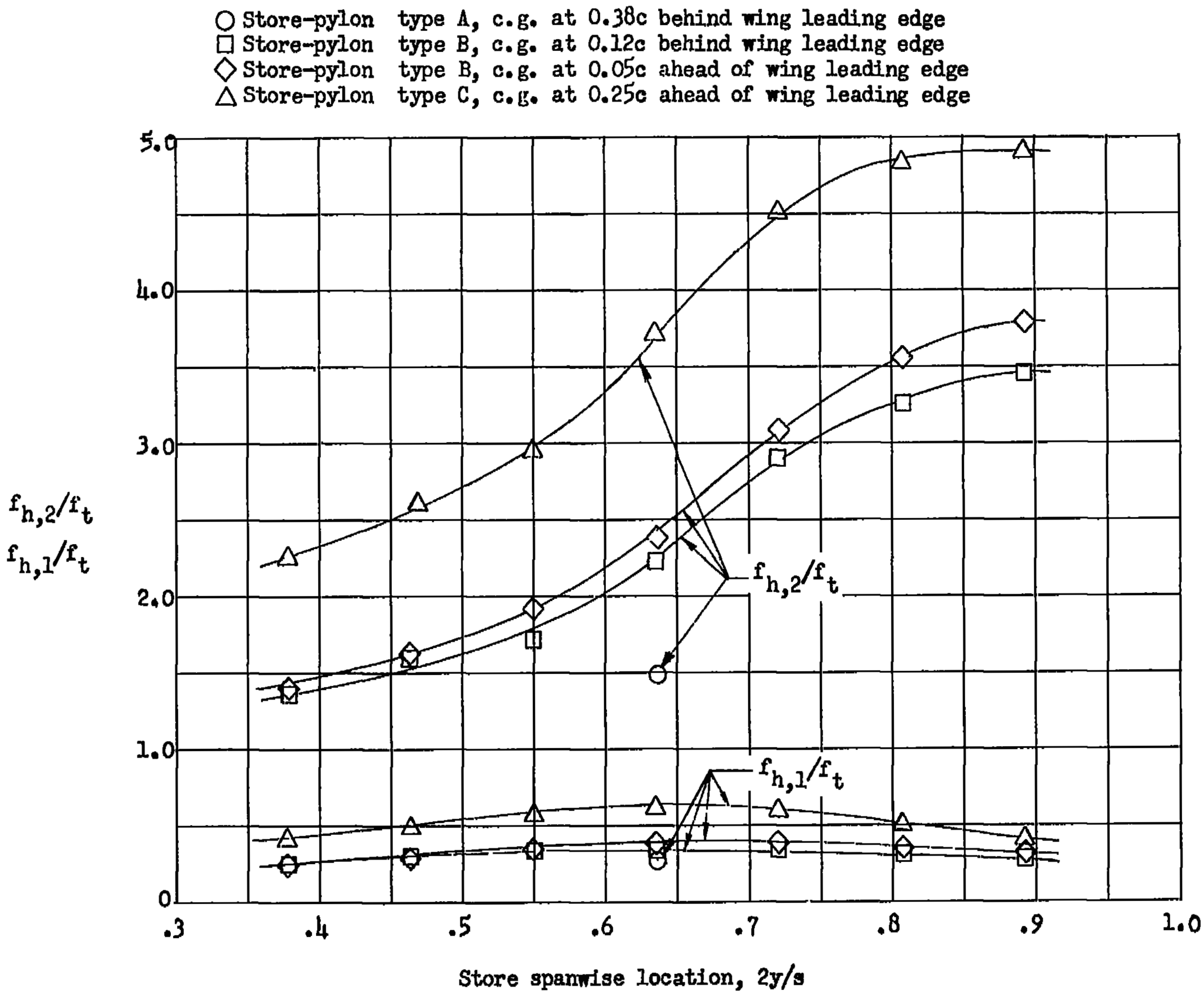

Figure 9.- Variation of frequency spectrum with spanwise location of stores.